Journal of The
Electrochemical Society

Molybdenum Sulfide within a Metal–Organic Framework for Photocatalytic Hydrogen Evolution from Water

JES Focus Issue on Semiconductor Electrochemistry and Photoelectrochemistry in Honor of Krishnan Rajeshwar

Molybdenum Sulfide within a Metal–Organic Framework for Photocatalytic Hydrogen Evolution from Water

Hyunho Noh,[1] Ying Yang,[1] Sol Ahn,[2] Aaron W. Peters,[1] Omar K. Farha,[1,2] and Joseph T. Hupp[1,*,z]

[1]*Department of Chemistry, Northwestern University, Evanston, Illinois 60208, USA*
[2]*Department of Chemical and Biological Engineering, Northwestern University, Evanston, Illinois 60208, USA*

A representative metal–organic framework, NU-1000, was functionalized with MoS_x. The previously determined crystal structure of the material, named **MoS_x-SIM**, consists of monometallic Mo(IV) ions with two sulfhydryl ligands. The metal ions are anchored to the framework by displacing protons presented by the –OH/–OH_2 groups on the Zr_6 node. As shown previously, the MOF-supported complexes are electrocatalytic for hydrogen evolution from acidified water. The earlier electrocatalysis results, together with the nearly ideal formal potential of the Mo(IV/II) couple (i.e., nearly coincident with that of the hydrogen couple), and the physical proximity of UV-absorbing MOF linkers to the complexes, suggested to us that the linkers might behave photosensitizers for catalyst reduction, and subsequently, for H_2 evolution from water. To our surprise, **MoS_x-SIM**, when UV-illuminated in an aqueous buffer at near-neutral pH, displays a biphasic photocatalytic response: an initially slow rate of reaction, i.e. 0.56 mmol g^{-1} h^{-1}, followed by an increase to 4 mmol g^{-1} h^{-1}. Ex-situ catalyst examination revealed that nanoparticulate MoS_x suspended within the reaction mixture is the actual catalyst. Thus, photo-assisted restructuring and detachment of the catalyst or pre-catalyst from the MOF node appears to be necessary for the catalyst to reduce water at neutral pH.

 [DOI: 10.1149/2.0261905jes]

Manuscript submitted November 12, 2018; revised manuscript received January 11, 2019. Published January 24, 2019. *This paper is part of the JES Focus Issue on Semiconductor Electrochemistry and Photoelectrochemistry in Honor of Krishnan Rajeshwar.*

Molecular hydrogen is a compound of undeniable global importance given its high demand as a feedstock in the industrial scale production of hydrocarbons and ammonia (i.e. Fisher-Tropsch and Haber-Bosch processes, respectively)[1–5] and as a reactant in fuel cells,[6,7] a technology of existing and increasing commercial significance. The overwhelming majority of commercially used H_2 is obtained by methane steam reforming or coal gasification[8] – low-cost technologies that unfortunately are complicated by the formation of greenhouse gases, i.e. CO_2 and CO.[9–11] In this regard, development of effective photo-,[12–15] electro-,[16–18] or photoelectrochemical hydrogen evolution catalysts[19–21] (i.e., by converting water into H_2) is of utmost interest. While the *in silico* predicted and experimentally proven effective catalysts typically contain of noble metals, most commonly platinum,[19,22] selected transition-metal chalcogenides, namely sulfides and selenides, have also proven functional as catalysts for the hydrogen evolution reaction (HER).[23,24] In particular, molybdenum disulfide has been extensively examined as an HER catalyst given its anomalous morphology-activity relationships. Experimental work by Jaramillo et al.,[24] and computational studies by Tsai et al.,[23,25] show that the catalysis primarily happens at the undercoordinated Mo sites (that form molybdenum-hydride species during the catalysis) solely presented at the so-called "crystallographic edge sites." Thus, amorphization of MoS_x materials has been used as a strategy to increase the surface density of the edge sites and thus increase the catalytic performance compared to crystalline catalysts.[26–28] Unfortunately, the structural ambiguity of amorphous materials makes difficult the quantitative exploration of potentially mechanistically instructive structure-activity relationships.

We propose crystalline metal–organic frameworks (MOFs) as an attractive and well-defined platform for satisfying the aforementioned criteria. MOFs that present a high density of labile protons, typically in the form of –OH/–OH_2 groups ligated to metal-oxo nodes, are of particular interest. We have reported elsewhere that post-synthetic exposure of MOF-node-sited aqua and hydroxo groups to highly reactive metal complexes (for example, metal alkyls), either in the vapor phase or inert condensed phase (e.g., heptane), results in their chemical attachment to the node – often as polynuclear clusters. Subsequent exposure to water vapor or H_2S converts the attached species to oxy- or mixed oxy-, sulfur-ligated complexes.[14,18,29–31] If the MOF nodes are viewed as tiny fragments of metal-oxides, the MOF-supported catalysts obtained by the aforementioned methods can be viewed as structurally well-defined, functional models of known or not-yet-discovered heterogeneous chemical catalysts or electrocatalysts. Envisioning a metal-chalcogenide-based photocatalyst, we selected a particular MOF, NU-1000, as a candidate support. NU-1000 consists of $Zr_6(\mu_3\text{–}O)_4(\mu_3\text{–}OH)_4(H_2O)_4(OH)_4$ nodes connected by 1,3,5,8-(*p*-benzoate)pyrene linkers. Upon irradiation with UV light, the linkers can be readily electronically excited and thereby enticed to function as redox-type photosensitizers (Figure 1).[32] The highly porous nature of NU-1000 facilitates introduction of metal complexes to the periodic arrays of –OH/–OH_2 nodes; the reactive complexes can be introduced either via vapor-phase atomic-layer-deposition-like (**A**LD-like) chemistry **i**n **M**OFs (AIM)[14,33] or **s**olvothermal **i**nstallation in **M**OFs (SIM).[18,29,31,34] We have previously shown that structures of the metal oxide and sulfide clusters can be readily interrogated via X-ray methods.[18,35]

The structure of MoS_x-modified NU-1000, here onwards named **MoS_x-SIM**, is of interest given its monometallic nature with mixed oxygen/sulfur coordination; it features sulfhydryl groups as well as oxo and hydroxo ligands originating from the node (Figure 1). The sulfhydryl groups (-SH ligands) constitute a possible of protons that can react with metal-bound hydrides to form molecular hydrogen. The structure of **MoS_x-SIM** is reminiscent of that of the aforementioned catalytically active MoS_2 edge sites. We have previously observed that **MoS_x-SIM** can function as a reductive electrocatalyst for generation of H_2 from acidified water, where facilitating features include the good hydrothermal stability of the parent framework[36] and the retention of MOF mesoporosity (27 Å mesopore diameter for **MoS_x-SIM** versus to 31 Å for NU-1000).[18] (Additionally, the sulfhydryl groups (-SH ligands) constitute a possible of protons that can react with metal-bound hydrides to form molecular hydrogen.) Notably, the formal potential of the monometallic molybdenum-sulfur catalyst was observed to be nearly coincident with that of the hydrogen couple (i.e. –20 mV vs. reversible hydrogen electrode or RHE). Given the electrically insulating nature of the framework,[37] various molecular redox-mediators or shuttles were enlisted and introduced into the solution permeating the electrode-supported, catalytic MOF. The

*Electrochemical Society Member.
zE-mail: j-hupp@northwestern.edu

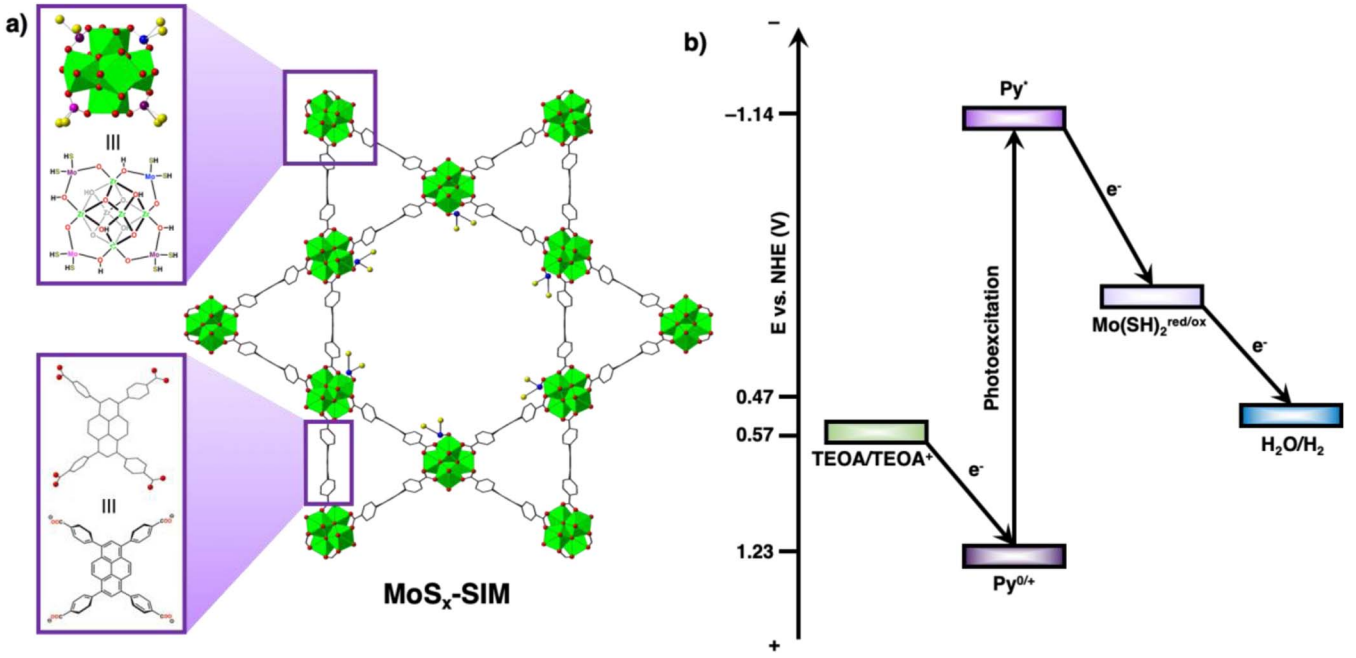

Figure 1. a) Crystallographic structure of **MoS_x-SIM** with the corresponding $Mo(SH)_2$-ligated node (different colors on Mo indicate crystallographically distinct Mo ions as described previously[18]) and the pyrene(Py)-based organic linker. b) Schematic representation of the proposed photocatalytic system using triethanolamine (TEOA) as the sacrificial electron donor.

mediators served to deliver reducing equivalents to otherwise electrochemically non-addressable units sited far from the underlying electrode. In principle, the reducing equivalents could be more effectively delivered, and the anchored catalysts more uniformly or completely utilized, by photo-exciting and then employing as regenerable photoreductants, the tertraphenylpyrene linkers.[14] (Electronic structure calculations place the energy of the lowest unoccupied molecular orbital (LUMO) of the framework-sited at –1.14 V vs. the normal hydrogen electrode (NHE).[38]) An analogous NiS_x-functionalized version of NU-1000 – albeit, featuring tetra-metal clusters rather than single metal ions – has been observed to be photocatalytically active for hydrogen evolution from an aqueous solution buffered at near-neutral pH.[14] Thus, we sought to evaluate the photocatalytic properties of **MoS_x-SIM** under identical reaction conditions. We found, in contrast to the electrocatalytic behavior of the material in acidified water,[18] irradiated **MoS_x-SIM** in near-neutral water undergoes a structural change that boosts its catalytic activity by an order of magnitude. As noted below, via post-catalysis characterization, we believe the monometallic units undergo photo-redox-induced detachment from the MOF node, together with consolidation of the released units into a nanoparticulate (i.e., multimetallic) molybdenum-sulfur suspension in solution. The MOF itself remains intact and serves as a photo-senzitizer for reduction of water to H_2 by the catalytic suspension.

Experimental

MoS_x-SIM was prepared and characterized according to the literature procedure.[18] Photocatalytic HER was performed in a pH 7 adjusted 1 M tris(hyrdoxymethyl)aminomethane (Tris) buffer, a condition analogous to that reported previously by Peters et al.[14] All pH measurements were conducted with the Oakton pH meter calibrated with the relevant buffer standards. 2 mg of **MoS_x-SIM** and a stir bar were placed and sealed inside a 10–20 mL microwave vial (Biotage) inside an argon-filled glove box. The system was subsequently removed from the glove box. Separately, 5 mL of 1 M Tris buffer and 0.25 mL of triethanolamine (TEOA) were charged into another 10–20 mL microwave vial. The solution was purged under argon for 20 min followed by an injection of all the solution to the vial containing the catalyst. The reaction mixture was briefly sonicated for catalyst dispersion and was irradiated with ∼0.5 W/cm^2 UV LED (λ_{max} = 390 nm; note the photochemical setup is analogous to that described before[39]) under stirring. At 2, 5, 10, 30, 60, and 120 minutes, the head-space gas composition was analyzed via 200 μL injection into the gas chromatography (Agilent 7890A GC system; see endnote for details[40]). After 120 min, the reaction mixture was centrifuged to collect the catalyst, which was washed extensively with water, subsequently with acetone, and was dried under vacuum at 80°C for post-catalysis characterization. Those include inductively coupled plasma optical emission spectroscopy (ICP-OES; Varian Vista-MDX model), transmission electron microscopy (TEM; Hitachi HD2300 STEM with copper mesh sample holder at 200 kV), and powder X-ray diffraction (PXRD) pattern measurements (Rigaku ATX-G). When testing the HER performance of the leached catalysts, after two hours of UV irradiation, the MOF crystallites were removed via centrifugation and further filtration of the aliquot through polyvinylidene fluoride syringe filter having 0.45 μm diameter pores (Fisher Scientific). Dynamic light scattering (DLS; Brookhaven BI-200 goniometer equipped with BI-9000 high speed correlators and 3 W Ar ion laser at 514 nm) experiments were conducted on the filtrate to determine the average size of the MoS_x agglomerates. To assess the activity of the leached catalyst, the filtered aliquot and the bare NU-1000 (1.6 mg for equimolar amount of the pyrene linker) were further charged into a 10–20 mL microwave vial, purged with Ar for another 20 min, and then irradiated with the same UV source with stirring for an additional 60 min.

Results and Discussion

Following UV light irradiation for 120 min on **MoS_x-SIM** in a pH 7 Tris buffer with TEOA as the sacrificial electron donor, H_2 was detected (Figure 2). The total yield reaches 7.6 ± 0.7 mmol g^{-1} (corresponding to turnover number (TON) of 3.7 ± 0.3 taking all catalytic species within the reaction vessel into consideration). These observations are consistent with electron transfer from photo-excited linkers to $Mo(SH)_2$ as an essential step for photo-catalysis, where the electron transfer is rendered irreversible by the sacrificial electron donor; see Figure 1b. Notably, in the absence of either TEOA or UV illumination, no detectable hydrogen is produced. (For experiments

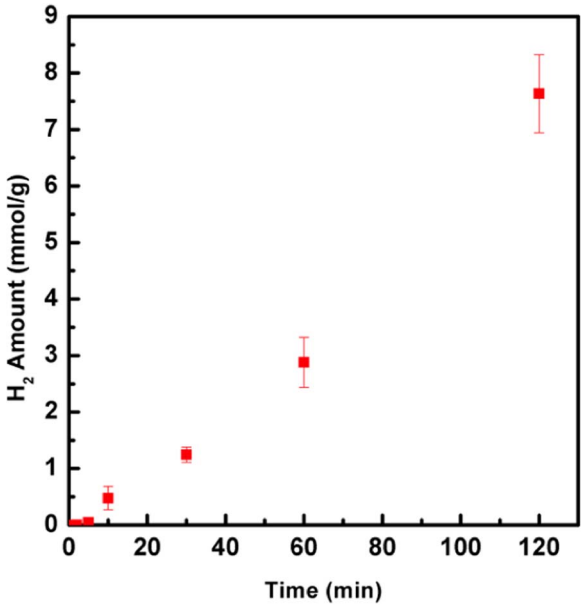

Figure 2. Photocatalytic H_2 evolution using **MoS_x-SIM** under UV light in a 1 M Tris buffer solution.

in the absence of TEOA, the pH of the 1 M Tris buffer was adjusted to pH = 8, thus matching that of TEOA-containing solutions.)

The molybdenum oxide derivative (here onwards named **MoO_x-SIM**) synthesized according to the reported procedure[31] and having the crystallographically determined structure reported previously,[18] yielded only tiny amounts of H_2 when subjected to UV irradiation in the presence of TEOA; see Table I. Thus, sulfidation appears to be necessary in order to generate a significantly active catalyst. We note that the formal potential of **MoO_x-SIM** was previously measured to be –10 mV vs. RHE,[18] a value that is similar to that for **MoS_x-SIM**. However, we have previously shown that Mo(VI) oxide is reduced to Mo(IV) upon exposure to H_2S and recruitment of sulfhydryls as ligands.[18] The metal centers in **MoO_x-SIM**, which are noncatalytic for hydrogen evolution, presumably cycle between oxidation states VI and IV, whereas the metal centers in **MoS_x-SIM** cycle between oxidation states IV and II. Peters, et al. have previously shown that the unmodified (i.e. molybdenum-free) MOF is not catalytic/photocatalytic for the HER.[14]

Notably for **MoS_x-SIM**, an induction period of about five minutes was observed, during which molecular hydrogen evolved at a comparatively slow rate, i.e., 0.56 ± 0.02 mmol g^{-1} h^{-1}. After 5 min, steady (or possibly accelerating) H_2 production at an average rate of 4.1 ± 0.3 mmol g^{-1} h^{-1} was observed. These observations suggest that the initially installed $Mo(SH)_2$ units undergo photo-redox driven chemical and structural changes before displaying significant catalytic activity.

An ICP-OES measurement of the post-catalysis sample revealed that only 0.7 ± 0.1 Mo remained attached to the Zr_6 node compared to the 2.7 ± 0.2 Mo/Zr_6 in the freshly prepared sample. The average number of S-based ligands on each Mo also decreased from 2.5 ± 0.2 to 0.7 ± 0.2. While the TEM images of the composite after catalysis reveal no detectable nanoparticle formation within the framework, and the bulk crystallinity of the material after catalysis is retained as evidenced by PXRD measurements (Figures 3a–3b,3d),[36] the leached catalyst conceivably may serve as an HER catalyst in solution. To gauge this possibility, after two hours of UV irradiation the molybdenum-depleted MOF crystallites were isolated (see the Experimental section for details). To the filtrate, fresh NU-1000 (molybdenum-free) was added as a light harvester and the combination was further irradiated. After one hour, 10.37 ± 0.03 μmol H_2 was found in the headspace gas. If, for simplicity, we assume that all of the leached $Mo(SH)_2$ (i.e., ∼74% of the amount initially present in the **MoS_x-SIM** sample) contributes to formation of catalytically active particles in solution, the H_2 yield translates to a TON of 6.21 ± 0.02 (H_2 molecules) on a per-molybdenum-atom basis and a TOF of 6.21 ± 0.02 h^{-1}. Dynamic-light-scattering measurements further suggests the agglomeration of the leached MoS_x is the DLS plot (Figure 3c) where ∼ 1 nm particles were observed within the filtrate collected after 2 hr of UV irradiation. The combined observations imply that, in contrast to the behavior observed earlier **MoS_x-SIM** in aqueous acid,[18] the initially deposited monometallic $Mo(SH)_2$ units are, at pH = 8, ineffective as catalysts and unstable (under illumination) toward detachment from the MOF and agglomeration into multinuclear molybdenum species in solution. The agglomerated objects, however, are effective for linker-excitation-facilitated reduction of water to H_2.

Conclusions

MoS_x-SIM, consisting of monometallic $Mo(SH)_2$ units grafted to the zirconia-like nodes of NU-1000, has previously been shown to be competent as an electrocatalyst for evolution of molecular hydrogen from aqueous acid solutions. We find that the same material in near-neutral (pH = 8) buffered aqueous solution is *photo*catalytic for hydrogen evolution when a sacrificial electron donor (TEOA) is present. The tetraphenyl-pyrene linkers of NU-1000 serve as light harvesters; in photo-excited form they behave as strong reductants and deliver electrons to the molybdenum sites, which ultimately catalyze the reduction of water to H_2. Notably, the photocatalysis is characterized initially and for the first few minutes by comparatively slow H_2 production, but subsequently by much faster production (roughly an order of magnitude faster). Concomitant with photolysis, molybdenum and sulfur are lost from the MOF and transferred to the external solution. We find that the expelled material, suspended or dissolved in solution, is effective for hydrogen evolution and that the catalysis can be photo-sensitized by introducing fresh molybdenum-free NU-1000 as a light harvester. Together with previously published results (mediated electrocatalysis) on **MoS_x-SIM** in aqueous acid, the new findings underscore the potential role of the reaction medium in stabilizing or destabilizing catalysts or pre-catalysts. They also underscore the potential for catalytically ineffective chemical units (pre-catalysts) to evolve into materials that are significantly more competent as catalysts for a given reaction. Given the role of metal-chalcogen clusters

Table I. Catalytic performance of MoS_x-SIM and MoO_x-SIM subjugated under various reaction conditions.

			Initial Rate[b]		Average Rate following five-minute induction period[c]		H_2 Yield after 120 min	
Sample	UV	TEOA	mmol g^{-1} h^{-1}	(TOF)[a] h^{-1}	mmol g^{-1} h^{-1}	(TOF)[a] h^{-1}	mmol g^{-1}	(TON)[a]
MoS_x-SIM	+	+	0.56 ± 0.02	0.27 ± 0.01	4.1 ± 0.3	1.9 ± 0.2	7.6 ± 0.7	3.7 ± 0.3
MoS_x-SIM	+	–	–	–	0.30 ± 0.06	0.14 ± 0.03	0.6 ± 0.1	0.28 ± 0.06
MoS_x-SIM	–	+	–	–	–	–	0	0
MoO_x-SIM	+	+	–	–	0.23 ± 0.09	0.09 ± 0.03	0.5 ± 0.2	0.18 ± 0.07

[a]TOF and TON were determined by taking all oxide or sulfide species in the reaction vessel into consideration. The two values on the rate and TOF row indicate those measured: [b]during the 0–5 min induction period, and [c]after the induction period.

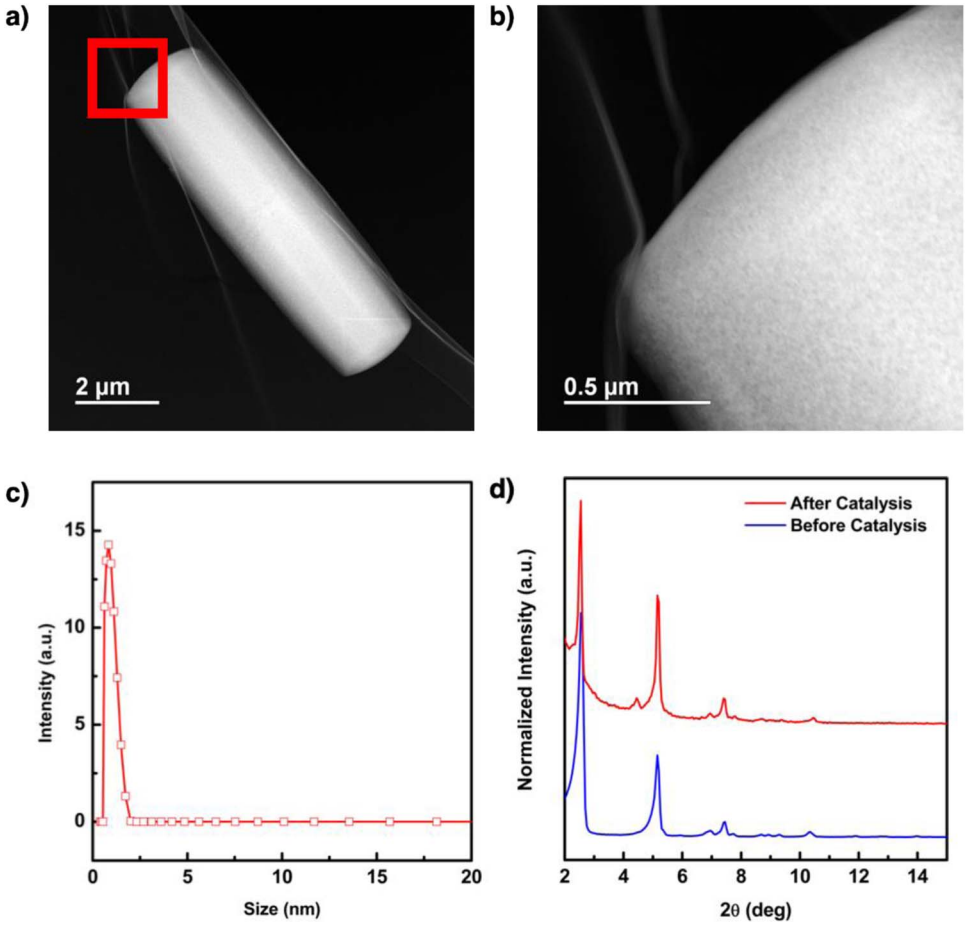

Figure 3. a) High resolution TEM images of the **MoS_x-SIM** after catalysis where the b) right image is the magnified image within the red box of the left image. c) DLS plot showing approximately 1 nm MoS_x agglomerates present within the filtrate after catalysis. d) PXRD pattern of **MoS_x-SIM** before and after catalysis, showing that the support retains its crystallinity.

as active sites for catalytic transformations of otherwise unreactive small molecules to more useful species (e.g., N_2 to ammonia in nitrogenase), we are optimistic that MOF-supported, reactant-accessible, chalcogen-containing multimetallic clusters, grown by SIM or related methods, can be deployed as electrocatalysts and/or photocatalysts for reactions more complex than HER and that structure-activity comparisons for families of such catalysts will prove mechanistically instructive. We intend to report shortly on our findings on both fronts.

Acknowledgments

This work was supported as part of the Center for Light Energy Activated Redox Processes (LEAP), an Energy Frontier Research Center funded by the U.S. Department of Energy, Office of Science, Basic Energy Sciences under Award # DE-SC0001059. H.N. gratefully acknowledges support from the Ryan Fellowship program of the Northwestern University International Institute of Nanotechnology. H.N. acknowledges Rebecca Palmer for her help in conducting dynamic light scattering experiment. This work made use of the J. B. Cohen X-ray Diffraction, EPIC, and KECK II facilities of Northwestern University's NUANCE Center, which has received support from the Soft and Hybrid Nanotechnology Experimental (SHyNE) Resource (NSF ECCS-1542205); the MRSEC program (NSF DMR1720139) at the Materials Research Center; the Institute for Nanotechnology (IIN); the Keck Foundation; and the State of Illinois, through the IIN. Finally, we thank UT Arlington Distinguished University Professor Raj Rajeshwar for his service to ECS and the photoelectrochemistry community, and to congratulate him on an extraordinary body of research accomplishments over the course of his first seventy years.

ORCID

Hyunho Noh https://orcid.org/0000-0003-3136-1004
Joseph T. Hupp https://orcid.org/0000-0003-3982-9812

References

1. H. Jahangiri, J. Bennett, P. Mahjoubi, K. Wilson, and S. Gu, *Catal. Sci. Technol.*, **4**, 2210 (2014).
2. A. Y. Khodakov, W. Chu, and P. Fongarland, *Chem. Rev.*, **107**, 1692 (2007).
3. M. E. Dry, *Catal. Today*, **71**, 227 (2002).
4. K. Timur, S. M. E., S. Anatoliy, B. Malte, and S. Robert, *Angew. Chem. Int. Ed.*, **52**, 12723 (2013).
5. A. R. Singh, B. A. Rohr, J. A. Schwalbe, M. Cargnello, K. Chan, T. F. Jaramillo, I. Chorkendorff, and J. K. Nørskov, *ACS Catal.*, **7**, 706 (2017).
6. J. Larminie and A. Dicks, *Fuel Cell Systems Explained*, John Wiley & Sons: West Sussex, (2003).
7. A. Kirubakaran, S. Jain, and R. K. Nema, *Renew. Sust. Energ. Rev.*, **13**, 2430 (2009).
8. J. M. Ogden, *Annu. Rev. Energy Env.*, **24**, 227 (1999).
9. N. S. Lewis and D. G. Nocera, *Proc. Natl. Acad. Sci. U. S. A.*, **103**, 15729 (2006).
10. A. A. Lacis, G. A. Schmidt, D. Rind, and R. A. Ruedy, *Science*, **330**, 356 (2010).
11. R. A. Betts, C. D. Jones, J. R. Knight, R. F. Keeling, and J. J. Kennedy, *Nat. Clim. Change.*, **6**, 806 (2016).
12. R. Kuriki, T. Ichibha, K. Hongo, D. Lu, R. Maezono, H. Kageyama, O. Ishitani, K. Oka, and K. Maeda, *J. Am. Chem. Soc.*, **140**, 6648 (2018).
13. L. Guo, Z. Yang, K. Marcus, Z. Li, B. Luo, L. Zhou, X. Wang, Y. Du, and Y. Yang, *Energy. Environ. Sci.*, **11**, 106 (2018).
14. A. W. Peters, Z. Li, O. K. Farha, and J. T. Hupp, *ACS Appl. Mater. Interfaces*, **8**, 20675 (2016).
15. D. Hong, Y. Yamada, M. Sheehan, S. Shikano, C.-H. Kuo, M. Tian, C.-K. Tsung, and S. Fukuzumi, *ACS Sustainable Chem. Eng.*, **2**, 2588 (2014).
16. A. B. Laursen, R. B. Wexler, M. J. Whitaker, E. J. Izett, K. U. D. Calvinho, S. Hwang, R. Rucker, H. Wang, J. Li, E. Garfunkel, M. Greenblatt, A. M. Rappe, and G. C. Dismukes, *ACS Catal.*, **8**, 4408 (2018).

17. D. V. Esposito, S. T. Hunt, A. L. Stottlemyer, K. D. Dobson, B. E. McCandless, R. W. Birkmire, and J. G. Chen, *Angew. Chem. Int. Ed.*, **49**, 9859 (2010).
18. H. Noh, C.-W. Kung, K.-I. Otake, A. W. Peters, Z. Li, Y. Liao, X. Gong, O. K. Farha, and J. T. Hupp, *ACS Catal.*, **8**, 9848 (2018).
19. Q. Ding, B. Song, P. Xu, and S. Jin, *Chem*, **1**, 699 (2016).
20. H. Hajibabaei, O. Zandi, and T. W. Hamann, *Chem. Sci.*, **7**, 6760 (2016).
21. C. Sheng, L. Wei, Y. Yanfa, H. Thomas, S. Ishiang, W. Dunwei, and M. Zetian, *Nano Futures*, **1**, 022001 (2017).
22. I. Roger, M. A. Shipman, and M. D. Symes, *Nat. Rev. Chem.*, **1**, 0003 (2017).
23. C. Tsai, K. Chan, F. Abild-Pedersen, and J. K. Norskov, *Phys. Chem. Chem. Phys.*, **16**, 13156 (2014).
24. T. F. Jaramillo, K. P. Jørgensen, J. Bonde, J. H. Nielsen, S. Horch, and I. Chorkendorff, *Science*, **317**, 100 (2007).
25. C. Tsai, F. Abild-Pedersen, and J. K. Nørskov, *Nano Lett.*, **14**, 1381 (2014).
26. Y. Guo, R. Wang, X. Xu, Y. Shang, and B. Gao, *Electrochim. Acta*, **273**, 402 (2018).
27. L.-A. Stern, P. Mocny, H. Vrubel, T. Bilgic, H.-A. Klok, and X. Hu, *ACS Appl. Mater. Interfaces*, **10**, 6253 (2018).
28. Z. Ji, C. Trickett, X. Pei, and O. M. Yaghi, *J. Am. Chem. Soc.*, (2018).
29. X. Zhang, Q. Hu, T. Xia, J. Zhang, Y. Yang, Y. Cui, B. Chen, and G. Qian, *ACS Appl. Mater. Interfaces*, (2016).
30. L. R. Parent, M. S. Denny, J. P. Patterson, P. Abellan, Q. M. Ramasse, F. Paesani, S. M. Cohen, and N. C. Gianneschi, *Microsc. Microanal.*, **24**, 1970 (2018).
31. H. Noh, Y. Cui, A. W. Peters, D. R. Pahls, M. A. Ortuño, N. A. Vermeulen, C. J. Cramer, L. Gagliardi, J. T. Hupp, and O. K. Farha, *J. Am. Chem. Soc.*, **138**, 14720 (2016).
32. J. E. Mondloch, W. Bury, D. Fairen-Jimenez, S. Kwon, E. J. DeMarco, M. H. Weston, A. A. Sarjeant, S. T. Nguyen, P. C. Stair, R. Q. Snurr, O. K. Farha, and J. T. Hupp, *J. Am. Chem. Soc.*, **135**, 10294 (2013).
33. I. S. Kim, Z. Li, J. Zheng, A. E. Platero-Prats, A. Mavrandonakis, S. Pellizzeri, M. Ferrandon, A. Vjunov, L. C. Gallington, T. E. Webber, N. A. Vermeulen, R. L. Penn, R. B. Getman, C. J. Cramer, K. W. Chapman, D. M. Camaioni, J. L. Fulton, J. A. Lercher, O. K. Farha, J. T. Hupp, and A. B. F. Martinson, *Angew. Chem. Int. Ed.*, **57**, 909 (2018).
34. S. Ahn, N. E. Thornburg, Z. Li, T. C. Wang, L. C. Gallington, K. W. Chapman, J. M. Notestein, J. T. Hupp, and O. K. Farha, *Inorg. Chem.*, **55**, 11954 (2016).
35. K.-I. Otake, Y. Cui, C. T. Buru, Z. Li, J. T. Hupp, and O. K. Farha, *J. Am. Chem. Soc.*, **140**, 8652 (2018).
36. A. J. Howarth, Y. Liu, P. Li, Z. Li, T. C. Wang, J. T. Hupp, and O. K. Farha, *Nat. Rev. Mater.*, **1**, 15018 (2016).
37. C.-W. Kung, A. E. Platero-Prats, R. J. Drout, J. Kang, T. C. Wang, C. O. Audu, M. C. Hersam, K. W. Chapman, O. K. Farha, and J. T. Hupp, *ACS Appl. Mater. Interfaces*, **10**, 30532 (2018).
38. C.-W. Kung, K. Otake, C. T. Buru, S. Goswami, Y. Cui, J. T. Hupp, A. M. Spokoyny, and O. K. Farha, *J. Am. Chem. Soc.*, **140**, 3871 (2018).
39. C. T. Buru, M. B. Majewski, A. J. Howarth, R. H. Lavroff, C.-W. Kung, A. W. Peters, S. Goswami, and O. K. Farha, *ACS Appl. Mater. Interfaces*, **10**, 23802 (2018).
40. Amount of H_2 was analyzed via GC equipped with a thermal conductivity detector (TCD) and a ultrahigh purity argon as the carrier gas. The headspace gas was passed through combination of two columns (column 1: HP-Plot Q, column 2: HP-Plot Molesieve) and the amount of H_2 was quantified by comparing the experimental results to the relevant calibration data.